

# Structural transition and atomic ordering in the non-stoichiometric double perovskite $\text{Sr}_2\text{Fe}_x\text{Mo}_{2-x}\text{O}_6$

G.Y. Liu<sup>a</sup>, G.H. Rao<sup>a,\*</sup>, X.M. Feng<sup>a</sup>, H.F. Yang<sup>a</sup>, Z.W. Ouyang<sup>a</sup>, W.F. Liu<sup>a</sup>, J.K. Liang<sup>a,b</sup>

<sup>a</sup>Institute of Physics and Center for Condensed Matter Physics, Chinese Academy of Sciences, Beijing 100080, PR China

<sup>b</sup>International Center for Materials Physics, Chinese Academy of Sciences, Shenyang 110015, PR China

Received 25 October 2002; accepted 4 November 2002

## Abstract

The structural transition and atomic ordering of a new series of ordered double perovskite oxides  $\text{Sr}_2\text{Fe}_x\text{Mo}_{2-x}\text{O}_6$  ( $0.8 \leq x \leq 1.5$ ) have been studied by X-ray powder diffraction (XRD). Rietveld refinement of the powder diffraction profiles indicates that the crystal structure of the compounds  $\text{Sr}_2\text{Fe}_x\text{Mo}_{2-x}\text{O}_6$  changes from a tetragonal  $I4/mmm$  lattice to a cubic  $Fm\bar{3}m$  lattice around  $x = 1.2$  and the lattice parameters decrease slightly as Fe content increases. The degree of ordering in  $\text{Sr}_2\text{Fe}_x\text{Mo}_{2-x}\text{O}_6$  exhibits a maximal at  $x = 0.95$  and decreases as  $x$  deviates from 0.95.

© 2002 Elsevier Science B.V. All rights reserved.

**Keywords:** Transition metal compounds; Oxide materials; Crystal structure; X-ray diffraction

## 1. Introduction

Recently, a double-perovskite oxide system,  $\text{Sr}_2\text{FeMoO}_6$ , has become an important topic of scientific interest in view of its remarkable room-temperature low-field magnetoresistive properties [1–3].  $\text{Sr}_2\text{FeMoO}_6$  is an ordered double perovskite of the  $\text{A}_2\text{BB}'\text{O}_6$  type with Fe and Mo atoms alternating on the B and B' sites, respectively. The structure of  $\text{Sr}_2\text{FeMoO}_6$  was suggested to be either tetragonal  $I4/mmm$  ( $\sqrt{2}a_p \times \sqrt{2}a_p \times 2a_p$ ) [1,4] or cubic  $Fm\bar{3}m$  ( $2a_p \times 2a_p \times 2a_p$ ) [5] (where  $a_p$  is the unit cell of a primitive perovskite), based on X-ray and neutron powder diffraction.

Monte Carlo simulation and experiments indicated that the magnetic and electron transport properties of  $\text{Sr}_2\text{FeMoO}_6$  are strongly related to the degree of ordering of the compound [6–8]. Accordingly, a lot of studies had been done on Mo site or Fe site doping [9–13]. For the  $\text{Sr}_2\text{Fe}(\text{W}_{1-x}\text{Mo}_x)\text{O}_6$  system, Kobayashi et al. [9] and Sugata et al. [10] reported that the degree of B/B' ordering increases with increasing the content of W. Yuan et al. [13] found that the substitution of  $\text{Fe}^{3+}$  ions by  $\text{Cu}^{2+}$  ions

enhances the site location ordering of Fe, Cu, and Mo on the B/B' site for the high-doping-level samples in the  $\text{Sr}_2(\text{Fe}_{1-x}\text{Cu}_x)\text{MoO}_6$  system ( $x = 0.20, 0.25, 0.30$ ). Nevertheless, experimental observations [1,9,14] that the saturated magnetization of  $\text{Sr}_2\text{FeMoO}_6$  was usually smaller than the expected value of  $4 \mu_B$  indicate that mutual substitution between Fe and Mo could take place. Therefore, it would be interesting to investigate the stability and ionic ordering of the non-stoichiometry compounds  $\text{Sr}_2\text{Fe}_x\text{Mo}_{2-x}\text{O}_6$ .

## 2. Experimental

$\text{Sr}_2\text{Fe}_x\text{Mo}_{2-x}\text{O}_6$  ( $0.8 \leq x \leq 1.5$ ) compounds were synthesized by a solid-state reaction at high temperature with starting materials of analytically pure  $\text{SrCO}_3$ ,  $\text{Fe}_2\text{O}_3$ , and  $\text{MoO}_3$ . The starting materials corresponding to each composition were mixed and calcined at  $900^\circ\text{C}$  for 10 h in air. The resulting mixtures were pressed into pellets, sintered at  $1280^\circ\text{C}$  for 12 h in a stream of 5%  $\text{H}_2/\text{Ar}$  with intermediate grindings, and then quenched to room temperature.

X-ray powder diffraction (XRD) analysis of the samples has been carried out at room temperature using a Rigaku D/max 2500 diffractometer with Cu  $K\alpha$  radiation (50

\*Corresponding author. Tel.: +86-10-8264-9085; fax: +86-10-8264-9531.

E-mail address: ghrao@aphy.iphy.ac.cn (G.H. Rao).

kV  $\times$  250 mA) and a graphite monochromator. A step scan mode was employed with a step width of  $2\theta = 0.02^\circ$  and a sampling time of 1 s in the range of  $15^\circ \leq 2\theta \leq 100^\circ$ . The XRD pattern showed that the compounds with  $x \geq 0.9$  were single phase without detectable secondary phase or

impurity. When  $x < 0.9$ , trace amounts of insulating  $\text{SrMoO}_4$  (up to 5 wt.% for  $x = 0.8$ ) were observed in the XRD patterns. The Rietveld refinement program FullProf [15,16] was used to obtain the crystal structure information of  $\text{Sr}_2\text{Fe}_x\text{Mo}_{2-x}\text{O}_6$  ( $0.8 \leq x \leq 1.5$ ).

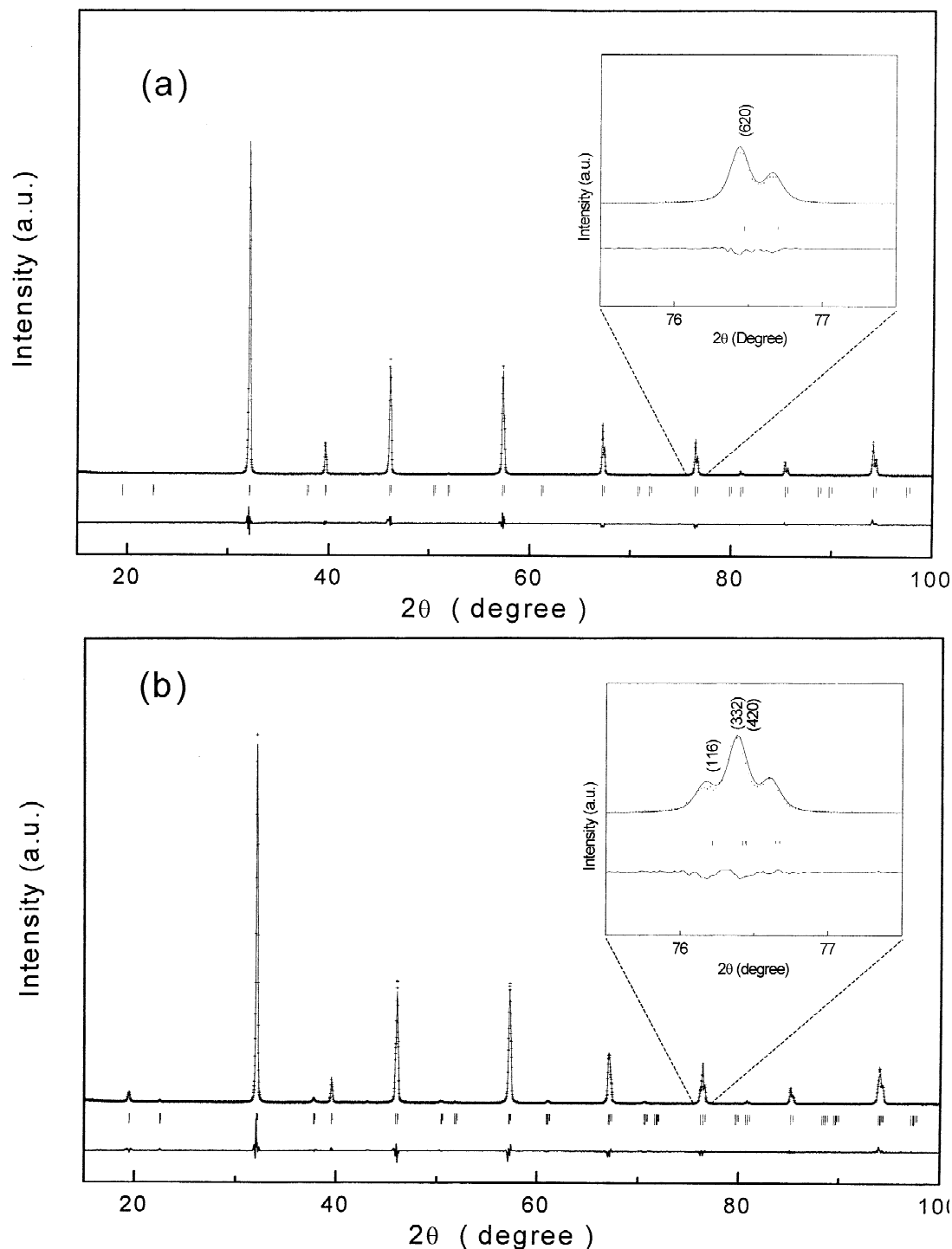


Fig. 1. Observed (crosses) and calculated (solid line) X-ray powder diffraction profiles of  $\text{Sr}_2\text{Fe}_x\text{Mo}_{2-x}\text{O}_6$  for (a)  $x = 1.5$  and (b)  $x = 1.05$ . The difference between the observed and calculated data is plotted at the bottom of each pattern. The small vertical bars mark the positions of expected reflections (the longer and short bars correspond to  $\text{K}\alpha_1$  and  $\text{K}\alpha_2$  radiations, respectively).

### 3. Results and discussion

#### 3.1. Crystal structure

We adopted the tetragonal structure with space group  $I4/mmm$  or the cubic structure with space  $Fm\bar{3}m$  as the initial structure to refine the XRD data of non-stoichiometry compounds  $\text{Sr}_2\text{Fe}_x\text{Mo}_{2-x}\text{O}_6$ . Rietveld refinement results, including lattice parameters and atomic parameters, are illustrated in Figs. 1 and 2 and Tables 1–3.

For the Fe-rich compounds ( $x=1.5$ , 1.4, and 1.3) in the  $\text{Sr}_2\text{Fe}_x\text{Mo}_{2-x}\text{O}_6$  system, the XRD data can be nicely fitted using the cubic  $Fm\bar{3}m$  model. The experimental and calculated patterns and the difference between them as well as the expected Bragg peak positions are shown in Fig. 1a for  $x=1.5$ . However, a tetragonal distortion takes place when  $x \leq 1.2$ , and the tetragonal  $I4/mmm$  model provides an excellent fit to the experimental data as shown in Fig. 1b for  $x=1.05$ . Thus, as the Fe content increases, the result of Rietveld analysis indicates the occurrence of a structural phase transition from the tetragonal  $I4/mmm$  ( $\sqrt{2}a_p \times \sqrt{2}a_p \times 2a_p$ ) lattice to the cubic  $Fm\bar{3}m$  ( $2a_p \times 2a_p \times 2a_p$ ) lattice around  $x=1.2$ . The structural transition is more evidenced by the splitting of the reflections, i.e. one reflection (620)C splits into three reflections of (116)T, (332)T, and (420)T as shown in Fig. 2 (see also the insets in Fig. 1, the doublet of (620)C results from the contribution of the doublet of  $K\alpha$  radiation).

Table 1

Lattice parameters and unit cell volume of the non-stoichiometric double perovskite  $\text{Sr}_2\text{Fe}_x\text{Mo}_{2-x}\text{O}_6$  system

Composition	Space group	$a$ (Å)	$c$ (Å)	$V$ (Å <sup>3</sup> )
$x=1.5$	$Fm\bar{3}m$	7.8717(1)	–	487.75
$x=1.4$	$Fm\bar{3}m$	7.8776(1)	–	488.85
$x=1.3$	$Fm\bar{3}m$	7.8798(1)	–	489.27
$x=1.2$	$I4/mmm$	5.5664(1)	7.8886(2)	488.86
$x=1.1$	$I4/mmm$	5.5659(2)	7.8929(3)	489.04
$x=1.05$	$I4/mmm$	5.5675(2)	7.8962(2)	489.52
$x=1.0$	$I4/mmm$	5.5693(1)	7.8983(3)	489.96
$x=0.95$	$I4/mmm$	5.5706(1)	7.8996(2)	490.26
$x=0.9$	$I4/mmm$	5.5714(2)	7.9007(3)	490.49
$x=0.8$	$I4/mmm$	5.5749(2)	7.9034(5)	491.26

Lattice parameters and unit-cell volume vs.  $x$  in  $\text{Sr}_2\text{Fe}_x\text{Mo}_{2-x}\text{O}_6$  ( $0.8 \leq x \leq 1.5$ ) are displayed in Fig. 3 and Table 1. The lattice parameters and the unit cell volume decrease slightly with the increase of composition  $x$  in  $\text{Sr}_2\text{Fe}_x\text{Mo}_{2-x}\text{O}_6$  ( $0.8 \leq x \leq 1.5$ ) in both the tetragonal phase region and the cubic phase region. Since the ionic radius of  $\text{Fe}^{3+}$  is larger than that of  $\text{Mo}^{5+}$ , this decrease might be attributed to cation or oxygen vacancies as observed in many perovskites [17–19] or valence disproportion. The valence disproportion is expected to fulfill the electro-neutrality in the compounds provided there are no cation and oxygen vacancies. Both the vacancy and valence disproportion could lead to the decrease of the unit cell volume with the increase of Fe content.

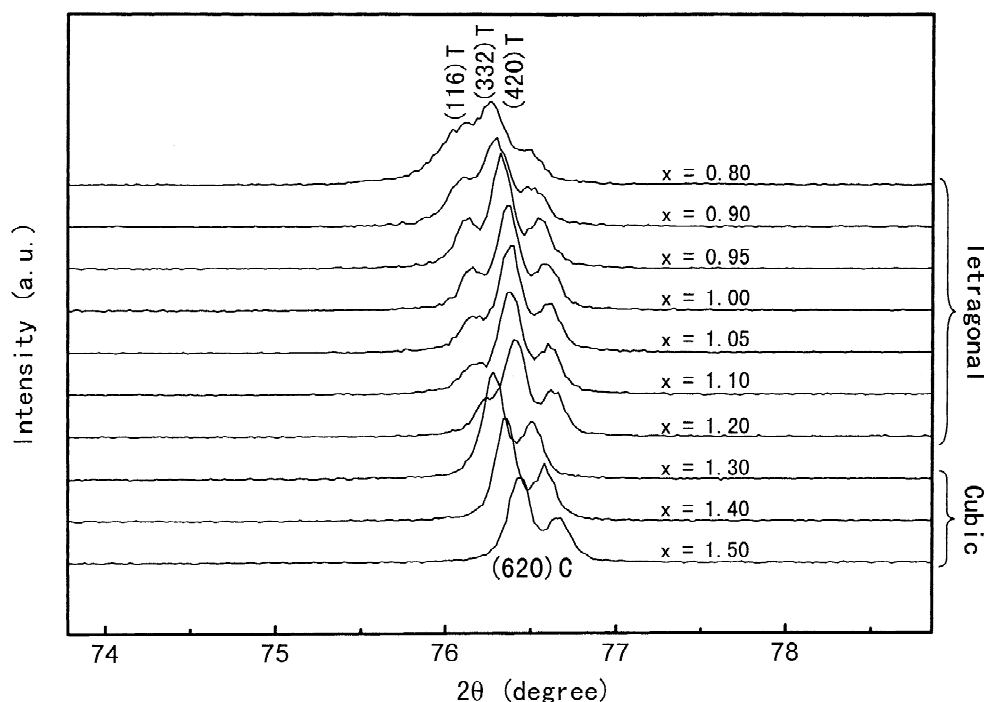


Fig. 2. Portion of the XRD patterns of  $\text{Sr}_2\text{Fe}_x\text{Mo}_{2-x}\text{O}_6$  showing the peak splittings (one peak of (620)C splits into three peaks of (116)T, (332)T, and (420)T) due to the structural phase transition from the tetragonal  $I4/mmm$  ( $\sqrt{2}a_p \times \sqrt{2}a_p \times 2a_p$ ) lattice in  $\text{Sr}_2\text{Fe}_x\text{Mo}_{2-x}\text{O}_6$  system to the cubic  $Fm\bar{3}m$  ( $2a_p \times 2a_p \times 2a_p$ ) lattice, where  $a_p$  is the unit cell of the primitive perovskite.

Table 2

Atomic parameters of the non-stoichiometric double perovskite  $\text{Sr}_2\text{Fe}_x\text{Mo}_{2-x}\text{O}_6$  ( $x > 1.2$ )

Atom		$x = 1.5$	$x = 1.4$	$x = 1.3$
Sr (8c)	$x$	0.25	0.25	0.25
	$y$	0.25	0.25	0.25
	$z$	0.25	0.25	0.25
	Occ.	1	1	1
Fe/Mo (4a)	$x$	0	0	0
	$y$	0	0	0
	$z$	0	0	0
	Occ. <sub>Fe</sub>	0.7402(127)	0.8454(68)	0.8923(53)
Mo/Fe (4b)	$x$	0	0	0
	$y$	0	0	0
	$z$	0.5	0.5	0.5
	Occ. <sub>Mo</sub>	0.2402(127)	0.4454(68)	0.5923(53)
O (24e)	$x$	0.2598(127)	0.1546(68)	0.1077(53)
	$y$	0	0	0
	$z$	0	0	0
	Occ.	1	1	1

### 3.2. Atomic ordering

In an ordered compound, the degree of ordering is a characterization of preferential occupation of different

atoms on respective sites in a unit cell. For a solid solution  $\text{A}_{1-x}\text{B}_x$  of an ordered phase AB, one can define the degree of ordering  $\eta$  as:  $\eta = P_A^{(1)} - P_A^{(2)} = P_B^{(2)} - P_B^{(1)}$ , where  $P_A^{(1)}$ ,  $P_A^{(2)}$ ,  $P_B^{(1)}$  and  $P_B^{(2)}$  are relative occupancies of A and B atoms on A site and B site respectively, i.e.  $P_A^{(1)} + P_B^{(1)} = 1$  and  $P_A^{(2)} + P_B^{(2)} = 1$ . Therefore, when complete disorder occurs,  $P_A^{(1)} = P_A^{(2)} = 1 - x$ ,  $P_B^{(1)} = P_B^{(2)} = x$ , and  $\eta = 0$ . When maximum ordering is achieved,  $P_A^{(1)} = 1$ ,  $P_A^{(2)} = 1 - 2x$ ,  $P_B^{(1)} = 0$ ,  $P_B^{(2)} = 2x$ , and  $\eta_{\max} = 2x$  for A-rich compounds ( $x \leq 0.5$ ), and  $P_B^{(2)} = 1$ ,  $P_B^{(1)} = 2x - 1$ ,  $P_A^{(1)} = 2(1 - x)$ ,  $P_A^{(2)} = 0$ , and  $\eta_{\max} = 2(1 - x)$  for B-rich compounds ( $x \geq 0.5$ ).

In the non-stoichiometric  $\text{Sr}_2\text{Fe}_x\text{Mo}_{2-x}\text{O}_6$ , Fe and Mo alternatively occupy the B and B' sites in a double perovskite  $\text{A}_2\text{BB}'\text{O}_6$ . Thus, based on the detailed quantitative Rietveld analysis of the XRD patterns, the degree of ordering  $\eta$  in non-stoichiometric double perovskite  $\text{Sr}_2\text{Fe}_x\text{Mo}_{2-x}\text{O}_6$  can be derived by  $\eta = \text{Occ}_{\text{Fe}}^{\text{B}} - \text{Occ}_{\text{Fe}}^{\text{B}'}$  ( $\text{Occ}_{\text{Fe}}^{\text{B}}$  and  $\text{Occ}_{\text{Fe}}^{\text{B}'}$  is the occupancy of Fe ions in B and B' sites, respectively). In Fig. 3, we show the derived  $\eta$  as a function of composition  $x$ . It is clearly indicated that the degree of the B/B'-site ordering is maximal about  $x = 0.95$  (approaches to  $\text{Sr}_2\text{FeMo}_2\text{O}_6$ ) and then decreases as  $x$

Table 3

Atomic parameters of the non-stoichiometric double perovskite  $\text{Sr}_2\text{Fe}_x\text{Mo}_{2-x}\text{O}_6$  ( $x \leq 1.2$ )

Atom	$x = 1.2$	$x = 1.1$	$x = 1.05$	$x = 1.0$	$x = 0.95$	$x = 0.9$	$x = 0.8$
Sr (4d)							
$x$	0.5	0.5	0.5	0.5	0.5	0.5	0.5
$y$	0	0	0	0	0	0	0
$z$	0.25	0.25	0.25	0.25	0.25	0.25	0.25
Occ.	1	1	1	1	1	1	1
Fe/Mo (2a)							
$x$	0	0	0	0	0	0	0
$y$	0	0	0	0	0	0	0
$z$	0	0	0	0	0	0	0
Occ. <sub>Fe</sub>	0.9093(53)	0.9048(49)	0.9071(43)	0.9197(42)	0.9125(42)	0.8651(43)	0.7259(61)
Occ. <sub>Mo</sub>	0.0907(53)	0.0952(49)	0.0929(43)	0.0803(42)	0.0875(42)	0.1349(43)	0.2741(61)
Mo/Fe (2b)							
$x$	0	0	0	0	0	0	0
$y$	0	0	0	0	0	0	0
$z$	0.5	0.5	0.5	0.5	0.5	0.5	0.5
Occ. <sub>Mo</sub>	0.7093(53)	0.8048(49)	0.8571(43)	0.9197(42)	0.9625(42)	0.9651(43)	0.9259(61)
Occ. <sub>Fe</sub>	0.2907(53)	0.1952(49)	0.1429(43)	0.0803(42)	0.0375(42)	0.0349(43)	0.0741(61)
O1 (8h)							
$x$	0.2533(17)	0.2538(14)	0.2546(12)	0.2536(12)	0.2530(12)	0.2563(13)	0.2444(12)
$y$	0.2533(17)	0.2538(14)	0.2546(12)	0.2536(12)	0.2530(12)	0.2563(13)	0.2444(12)
$z$	0	0	0	0	0	0	0
Occ.	1	1	1	1	1	1	1
O2 (4e)							
$x$	0	0	0	0	0	0	0
$y$	0	0	0	0	0	0	0
$z$	0.2436(30)	0.2465(27)	0.2517(24)	0.2536(22)	0.2568(21)	0.2472(20)	0.2665(25)
Occ.	1	1	1	1	1	1	1

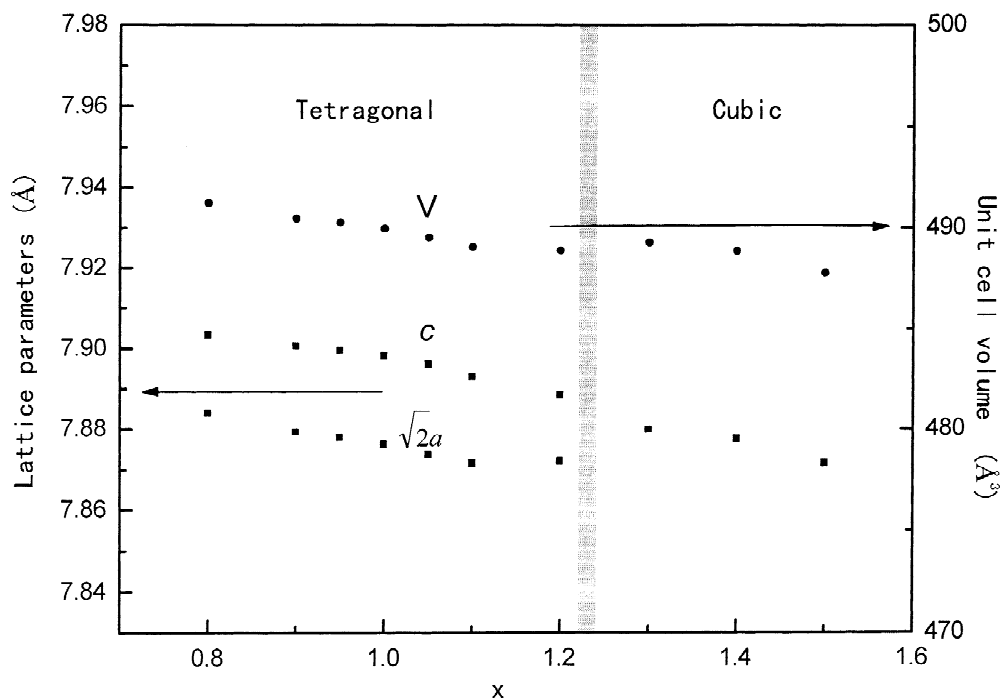


Fig. 3. Composition dependence of the lattice parameters and the unit-cell volume of  $\text{Sr}_2\text{Fe}_x\text{Mo}_{2-x}\text{O}_6$ . The phase boundary is a tentative one.

deviates from 0.95. It implies that a departure of  $x$  from 0.95 in the  $\text{Sr}_2\text{Fe}_x\text{Mo}_{2-x}\text{O}_6$  system tends to increase the disorder of the B/B'-site. The maximum degree of ordering  $\eta_{\max}$  ( $\eta_{\max} = 2-x$  for  $x \geq 1.0$  and  $\eta_{\max} = x$  for  $x < 1.0$ ) has also been shown as a function of  $x$  by the dash-dot line in Fig. 4. It is intriguing that  $\eta_{\max} - \eta \approx 0.18$  for

$1.0 \leq x \leq 1.2$  and  $\eta_{\max} - \eta \approx 0.075$  for  $0.8 \leq x \leq 0.95$ . It is worth noting that  $(\eta_{\max} - \eta)/2$  can be regarded as the actual antisite defect concentration  $\text{Occ}_{\text{Fe}}^{\text{B}'}(x \leq 1.0)$  or  $\text{Occ}_{\text{Mo}}^{\text{B}}(x \geq 1.0)$  in the non-stoichiometric double perovskite  $\text{Sr}_2\text{Fe}_x\text{Mo}_{2-x}\text{O}_6$ , i.e. if complete ordering occurred,  $\text{Occ}_{\text{Fe}}^{\text{B}'} = 0$  for  $x \leq 1.0$  and  $\text{Occ}_{\text{Mo}}^{\text{B}} = 0$  for  $x \geq 1.0$ . This

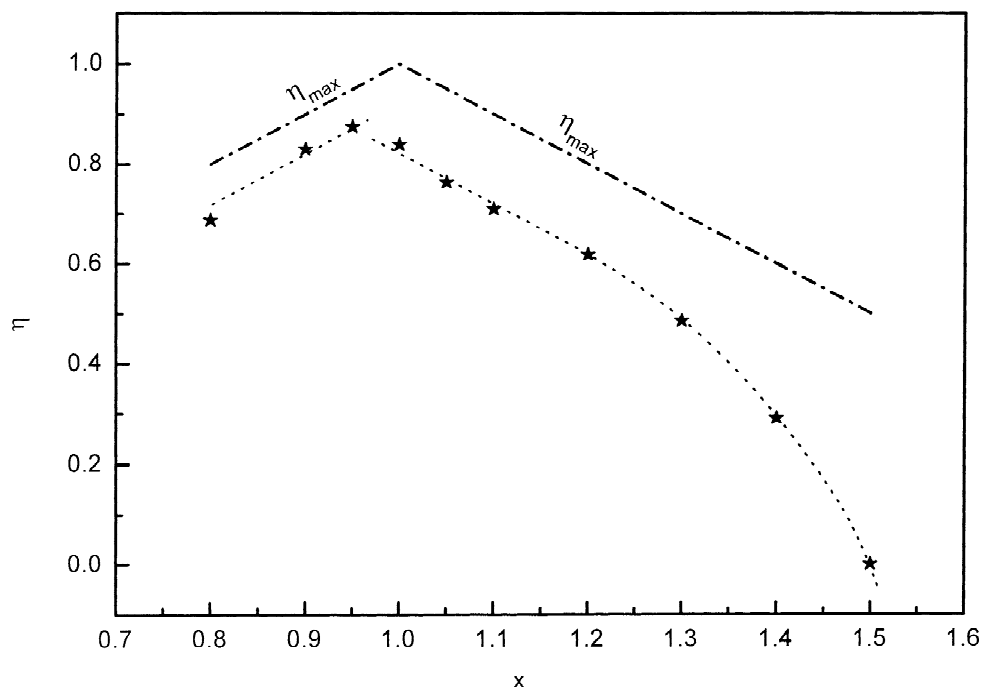


Fig. 4. Degree of ordering  $\eta$  as a function of  $x$  in non-stoichiometric double perovskite  $\text{Sr}_2\text{Fe}_x\text{Mo}_{2-x}\text{O}_6$  system. The dash-dot line indicates the expected maximum degree of ordering (see text). The dashed line is a guide to eyes.

observation seems to imply that an almost constant antisite defect concentration is necessary under our synthesis conditions to stabilize the tetragonal double perovskite  $\text{Sr}_2\text{Fe}_x\text{Mo}_{2-x}\text{O}_6$ . In addition, the required antisite defect concentration is about three times larger in Fe-rich compounds than that in Mo-rich compounds. The occurrence of the structural phase transition from the tetragonal lattice to the cubic lattice is evidenced by the rapid decrease of  $\eta$  when  $x > 1.2$ .

#### 4. Conclusion

In summary, the crystal structure of the non-stoichiometric  $\text{Sr}_2\text{Fe}_x\text{Mo}_{2-x}\text{O}_6$  system with ( $0.8 \leq x \leq 1.5$ ) is investigated. The alteration of the relative content between Fe and Mo in  $\text{Sr}_2\text{Fe}_x\text{Mo}_{2-x}\text{O}_6$  exhibits a significant effect on the crystal structure and the ionic ordering of the compounds. The degree of ordering is maximal at  $x = 0.95$  and decreases as  $x$  deviates from 0.95. A structural transition from the tetragonal  $I4/mmm$  lattice to the cubic  $Fm\bar{3}m$  lattice occurs around  $x = 1.2$ . It seems that an appropriate antisite defect is necessary to stabilize the double perovskite structure under our synthesis conditions.

#### Acknowledgements

This work is supported by the National Natural Foundation of China and State Key Project of Fundamental Research.

#### References

- [1] K.-I. Kobayashi, T. Kimura, H. Sawada, K. Terakura, Y. Tokura, *Nature* 395 (1998) 677.
- [2] D.D. Sarma, E.V. Sampathkumaran, S. Ray, R. Nagarajan, S. Majumdar, A. Kumar, G. Nalini, N.T. Guru-Row, *Solid State Commun.* 114 (2000) 465.
- [3] D.D. Sarma, P. Mahadevan, T. Saha-Dasgupta, S. Ray, A. Kumar, *Phys. Rev. Lett.* 85 (2000) 2549.
- [4] M. Itoh, I. Ohta, Y. Inaguma, *Mat. Sci. Eng. B* 41 (1996) 55.
- [5] B. García-Landa, C. Ritter, M.R. Ibarra, J. Blasco, P.A. Algarabel, R. Mahendiran, J. García, *Solid State Commun.* 110 (1999) 435.
- [6] A.S. Ogale, S.B. Ogale, R. Ramesh, T. Venkatesan, *Appl. Phys. Lett.* 75 (1999) 537.
- [7] M. García-Hernández, J.L. Martínez, M.J. Martínez-Lope, M.T. Casais, J.A. Alonso, *Phys. Rev. Lett.* 86 (2001) 2443.
- [8] L. Balcells, J. Navarro, M. Bibes, A. Roig, B. Martínez, J. Fontcuberta, *Appl. Phys. Lett.* 78 (2001) 781.
- [9] K.-I. Kobayashi, T. Okuda, Y. Tomioka, T. Kimura, Y. Tokura, *J. Magn. Magn. Mater.* 218 (2000) 17.
- [10] S. Ray, A. Kumar, S. Majumdar, E.V. Sampathkumaran, D.D. Sarma, *J. Phys.: Condens. Matter* 13 (2001) 607.
- [11] Y. Moritomo, H. Kusuya, T. Akimoto, A. Machida, *Jpn. J. Appl. Phys.* 39 (2000) L360.
- [12] F. Sriti, A. Maignan, C. Martin, B. Raveau, *Chem. Mater.* 13 (2001) 1746.
- [13] C.L. Yuan, Y. Zhu, P.P. Ong, *J. Appl. Phys.* 91 (2002) 4421.
- [14] R.P. Borges, R.M. Thomas, C. Cullinam, J.M.D. Coey, R. Ruryanarayanan, L. Ben-Dor, L. Pinsard-Gaudart, A. Revcolevschi, *J. Phys.: Condens. Matter* 11 (1999) L445.
- [15] H.M. Rietveld, *Acta Crystallogr.* 229 (1967) 151.
- [16] J.L. Rodríguez-Carvajal, *Physica B* 192 (1993) 55.
- [17] J. Töpfer, J.B. Goodenough, *Chem. Mater.* 9 (1997) 1467.
- [18] J.A.M. van Roosmalen, P. van Vlaanderen, E.H.P. Cordfunke, W.L. Ijdo, D.J.W. Ijdo, *J. Solid State Chem.* 114 (1995) 516.
- [19] Y. Takeda, K. Kanno, T. Takada, O. Yamamoto, M. Takano, N. Nakayama, Y. Bando, *J. Solid State Chem.* 63 (1986) 237.